CORE
Metadata, citation and similar papers at core.ac.uk
Provided by idUS. Depósito de Investigación Universidad de Sevilla

Journal of Applied Physics

Influence of plasma-generated negative oxygen ion impingement on magnetron sputtered amorphous SiO_2 thin films during growth at low temperatures

Cite as: J. Appl. Phys. **111**, 054312 (2012); https://doi.org/10.1063/1.3691950
Submitted: 08 November 2011 . Accepted: 03 February 2012 . Published Online: 08 March 2012

M. Macias-Montero, F. J. Garcia-Garcia, R. Álvarez, J. Gil-Rostra, J. C. González, J. Cotrino, A. R. Gonzalez-Elipe, and A. Palmero

View Online
Export Citation

ARTICLES YOU MAY BE INTERESTED IN

Influence of the negative oxygen ions on the structure evolution of transition metal oxide thin films
Journal of Applied Physics **100**, 023503 (2006); https://doi.org/10.1063/1.2216354

Microstructural evolution during film growth
Journal of Vacuum Science & Technology A **21**, S117 (2003); https://doi.org/10.1116/1.1601610

Modeling the flux of high energy negative ions during reactive magnetron sputtering
Journal of Applied Physics **106**, 093302 (2009); https://doi.org/10.1063/1.3247545

Challenge us.
What are your needs for periodic signal detection?
Zurich Instruments

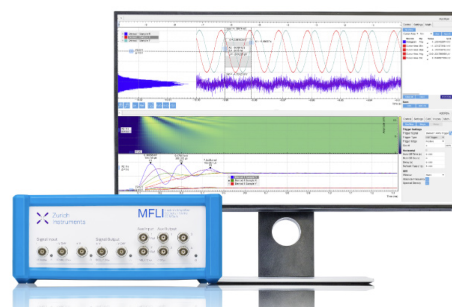

© 2012 American Institute of Physics.

Influence of plasma-generated negative oxygen ion impingement on magnetron sputtered amorphous SiO_2 thin films during growth at low temperatures

M. Macias-Montero,[1] F. J. Garcia-Garcia,[1] R. Álvarez,[1,a)] J. Gil-Rostra,[1] J. C. González,[1] J. Cotrino,[1,2] A. R. Gonzalez-Elipe,[1] and A. Palmero[1]

[1]*Instituto de Ciencia de Materiales de Sevilla (CSIC-US), Américo Vespucio 49, 41092 Seville, Spain*
[2]*Departamento de Física Atómica, Molecular y Nuclear, Universidad de Sevilla, Avda. Reina Mercedes, s/n, 42022 Seville, Spain*

(Received 8 November 2011; accepted 3 February 2012; published online 8 March 2012)

Growth of amorphous SiO_2 thin films deposited by reactive magnetron sputtering at low temperatures has been studied under different oxygen partial pressure conditions. Film microstructures varied from coalescent vertical column-like to homogeneous compact microstructures, possessing all similar refractive indexes. A discussion on the process responsible for the different microstructures is carried out focusing on the influence of (i) the surface shadowing mechanism, (ii) the positive ion impingement on the film, and (iii) the negative ion impingement. We conclude that only the trend followed by the latter and, in particular, the impingement of O^- ions with kinetic energies between 20 and 200 eV, agrees with the resulting microstructural changes. Overall, it is also demonstrated that there are two main microstructuring regimes in the growth of amorphous SiO_2 thin films by magnetron sputtering at low temperatures, controlled by the amount of O_2 in the deposition reactor, which stem from the competition between surface shadowing and ion-induced adatom surface mobility. © *2012 American Institute of Physics*. [http://dx.doi.org/10.1063/1.3691950]

I. INTRODUCTION

The interaction of plasma-generated species with a growing film in connection with the formation of a given microstructure has been a subject of an intensive research in the last decades in the field of reactive magnetron sputtering depositions (see, for instance, Refs. 1–6). This technique is one of the most popular in science and technology due to the high quality of the deposited films, the possibility to work on large substrates as well as to the high deposition rates achieved. Furthermore, the strongly coupled non-lineal phenomena governing the plasma/film interaction enable the growth of coatings with characteristic microstructures and singular properties that improve their performance and efficiency for many technological applications (see, for instance, Refs. 7–9). Some relevant scientific issues regarding the influence of the plasma on the film growth are linked to (i) cathode poisoning and process instability,[10,11] (ii) changes in the momentum and kinetic energy of the sputtered particles when arriving at the film due to scattering processes on plasma particles,[12–16] and (iii) positive and negative ion impingement on the film surface during growth.[17–21]

Cathode poisoning is an undesired effect that takes place when there is an excess of reactive gas in the deposition reactor. This poisoning alters the composition of the first monolayers of the sputter target, thus diminishing the sputtering rate and efficiency of the overall process. In the last decades much effort has been dedicated to reduce its influence, for instance, by varying the pumping speed, increasing the cathode-film distance, or by pulsing the reactive gas flow (see, for instance, Ref. 10, and references therein). Conversely, the surface shadowing mechanism, determined by the directionality of the sputtered particles arriving at the film, is a relevant process by which taller film surface features prevent the deposition under their shadow.[22] According to the structure zone model (SZM), the value of the ratio T_s/T_m (the so-called homologous temperature), where T_s is the film temperature during growth and T_m the melting temperature, gives information on the relevance of surface shadowing in comparison with thermally activated diffusion processes during growth.[23] In this way, when T_s/T_m is approximately below 0.3 (the so-called Zone I), the SZM indicates that surface shadowing dominates over thermally activated diffusion processes. On the other hand, for increasing values of T_s/T_m, thermally activated surface diffusion starts to play a role (the so-called T Zone), whereas for even higher values of T_s/T_m the diffusion of bulk atoms becomes dominant (Zone II).[23] Consequently, surface shadowing must be taken into account whenever the growth takes place in Zone I and T.

Positively charged ions, produced in the plasma bulk via electron-induced inelastic collisional processes, are accelerated by the electric field either toward the cathode, inducing the sputtering mechanism, or toward the film and reactor grounded regions with kinetic energies up to few tens of electronvolts.[24] On the other hand, the use of electronegative gases in the reactor enables the formation of negative ions, which are produced either by electron attachment in the plasma or by attachment of secondary electrons at the cathode surface.[25,26] Those produced in the plasma volume possess typical kinetic energies similar to those of the positive ions, whereas negative ones produced at the cathode surface are accelerated through the cathode sheath toward the plasma

a)Electronic mail: rafael.alvarez@icmse.csic.es.

 © 2012 American Institute of Physics

volume and may arrive at the film surface with kinetic energies of the order of the cathode potential fall (i.e., few hundred of electronvolts). In general, ion impingement on the film during growth induces, to a certain extent, adatom surface mobility that competes with the processes described in the SZM, producing the removal voids and the densification of the films.[18,23,27,28] Moreover, high energy ion impingement is also known for producing changes in the film texturing in crystalline materials, associated to locally ion-induced damage in the film network.[23] In Ref. 29, the flux of ions toward the material was measured by energy-resolved mass spectrometry in a dc magnetron discharge of Ar/O_2, using a cathode made of Si. Under the reported conditions, O^- was the most abundant type of negative ion species impinging onto the film, possessing an energy distribution characterized by a high energy peak at the cathode potential, and a low energy peak corresponding to the negative ions produced in the target region. Furthermore, some intermediate energy peaks were found associated to oxygen-containing negative molecules (O_2^-, SiO_2^-, SiO_3^-, etc.) that were produced at the cathode surface and subsequently dissociated in the plasma bulk. More recently, in Ref. 25, it was concluded that cathode poisoning was straightforwardly connected to the production of negative ions on the cathode surface and, thus, to the high energy negative ion bombardment during growth. This is of special relevance, as in Ref. 30 it was obtained that the impingement of high and intermediate energy O^- produced at the cathode surface influenced the crystallization degree of metal oxides.

In this paper we study the role of plasma-generated ion impingement during film growth by magnetron sputtering through the analysis of the microstructures of amorphous films deposited under selected experimental conditions and discuss its relevance in comparison with other competing processes. Due to its importance for many applications we have performed the present study with SiO_2 thin films: the results have shown a clear interdependence between the high energy negative ion impingement and film microstructure, which can be of general application for the growth of other metal oxide coatings.

II. EXPERIMENTAL SETUP

A cylindrical vacuum reactor was used for the experiments, pumped down to a base pressure below 10^{-4} Pa by a combination of turbomolecular and rotary pumps. The working gases used were a variable mixture of Ar (purity 99.995%) and O_2 (purity 99.995%), being the working pressure adjusted by a throttling valve between the chamber and the turbo pump. Amorphous SiO_2 thin films were deposited by reactive magnetron sputtering in the argon/oxygen atmosphere using a silicon planar target with a diameter of 50 mm and a thickness of 3 mm. Experiments were carried out using a magnetron driven by a pulsed unipolar dc power supply working in a frequency of 80 kHz, with a duty cycle of 40%, which indicated the averaged peak value of the cathode potential. Three different experimental conditions have been explored in this paper corresponding to different amounts of O_2 in the reactor, maintaining the argon partial pressure constant in all the cases (0.28 Pa). Deposition

TABLE I. Experimental conditions and obtained film thicknesses.

Conditions	Ar pressure (Pa)	O_2 pressure (Pa)	Total pressure (Pa)	Power (W)	Cathode potential (V)	Film thickness (nm)
High O_2	0.28	0.25	0.53	300	408	335
Intermediate O_2	0.28	0.09	0.37	300	421	380
Low O_2	0.28	0.02	0.3	100	406	300

parameters used in this work are shown in Table I. The evolution in time of the cathode potential is presented in Fig. 1 for the different experimental conditions. It is worthwhile to mention that, in the low O_2 case, the electromagnetic power applied is lower than in the other two cases to keep the source voltage at a similar range of values. Thin films were grown during 30 min by leaving the substrate holder at the floating potential (i.e., it was neither electrically biased nor grounded) and placing it at a distance of 70 mm from the cathode, being the temperature below 350 K in all the cases. An additional film, prepared for comparative discussions, was grown for 60 min under the same conditions as those in the high O_2 case in Table I, but at the backside of the substrate holder, not facing the cathode and the plasma.

Ion fluxes were measured using an energy-resolved mass spectrometer (EQP 500, Hiden Analytical Ltd). The EQP system directly measures mass and energy of both positive and negative ions in the plasma, detecting masses up to 510 amu and ion energies up to 1000 eV. The orifice (0.05 mm of diameter) of the spectrometer was positioned at a distance of 70 mm from the center of the target, at the same location where the substrates were placed during the depositions (see Fig. 2). Films were characterized through field emission scanning electron microscopy (FESEM), for which we grew a gold cap layer on top of each in order to increase image contrast. Measured film thicknesses are included in Table I. In addition, and in order to help the discussion, we further characterized the films by transmission infrared spectroscopy (IR), X-ray photoelectron spectroscopy (XPS), atomic force microscopy (AFM) and spectroscopic ellipsometry.

Spectroscopic ellipsometry was carried out in a J.A. Woollam VASE (variable angle spectroscopic ellipsometry) spectroscopic ellipsometer. Values of the ellipsometry

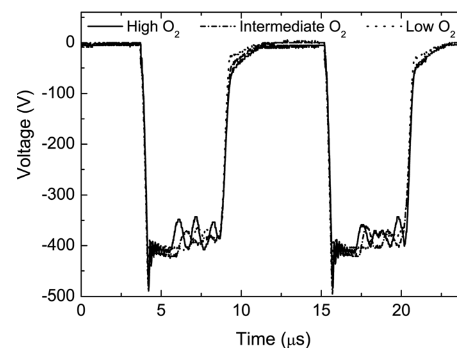

FIG. 1. Evolution in time of the cathode potential for the conditions described in Table I.

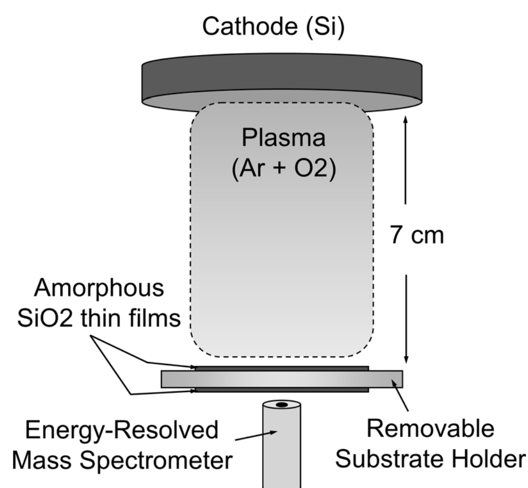

FIG. 2. Experimental setup. When the mass spectrometer is used for the analysis, the substrate holder is removed.

parameters (ψ and Δ) were obtained over the spectral range of 300 to 1000 nm, at 2 nm resolution. As a consistency checking parameter, the incidence angle was set at 65°, 70°, and 75°. Optical modeling and fitting parameters were obtained with the WASE32© program (J.A. Woollam Co., Inc.). Ellipsometry spectra were analyzed by knowing the film thickness and roughness (thickness values were obtained by the cross-section FESEM images, whereas the roughness was determined by AFM) and using a non-ideal model that took into account a possible non-uniformity of the film thickness and the angular spread of the beam entering the detector. Quality assessment of the fit data was done by minimizing the mean-square dispersion that was below 10 units in all the studied cases. The ellipsometric optical model consisted of the three following layers: (1) A rough surface layer, (2) a Bruggeman effective medium approximation layer, and (3) a Cauchy layer. The Bruggeman effective medium approximation, which represents the sample as a physical mixture of a continuous film with voids, was coupled to the Cauchy layer.[31]

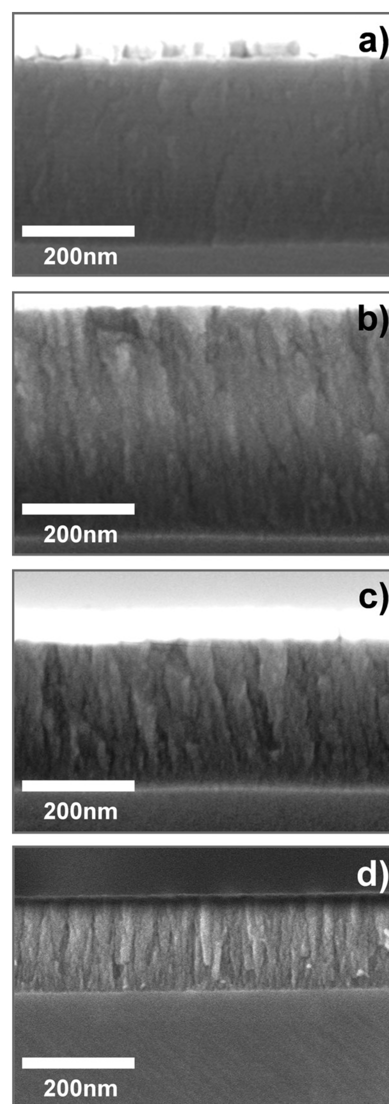

FIG. 3. Cross-sectional FESEM images of the films deposited under the conditions appearing in Table I: (a) High O_2 case, (b) intermediate O_2 case, (c) low O_2 case, and (d) film deposited at the backside of the substrate holder in the high O_2 case conditions.

III. RESULTS AND DISCUSSION

In Figs. 3(a)–3(c) we present the cross-sectional FESEM images of the three films deposited with different oxygen pressures in the reactor. Figure 3(a) shows that the film grown with the highest O_2 partial pressure possesses a homogeneous microstructure, with no geometrical pattern in the bulk. In Fig. 3(b), corresponding to the intermediate O_2 pressure case in Table I, the film presents a coalescent vertical column-like microstructure, which is more evident in the film deposited under the low O_2 pressure condition (Fig. 3(c)). In Fig. 3(d) we show the cross-sectional FESEM image of the SiO_2 thin film deposited at the back side of the substrate holder, where the growth takes place under very weak or no plasma ion impingement.[16] This assumption is supported by the experimental observation that no plasma glow develops at the back side of the substrate holder during the deposition. Although Si atoms directionality, and therefore the surface shadowing mechanism, is expected to be very different in this configuration, Fig. 3(d) shows that this film possesses a microstructure similar to those of the films deposited at intermediate and low O_2 pressure conditions (Figs. 3(b) and 3(c)). Hence, a qualitative trend can be observed: For lower O_2 partial pressures in the reactor, the observed film microstructures tend to resemble that of the film prepared at the backside of the substrate holder, grown under a weak influence of plasma ions.

The chemical composition of the films determined by XPS after surface cleaning by ion bombardment resulted to be SiO_2 in all the cases (data not shown). Meanwhile, the IR spectra (Fig. 4) of the three studied films in the region between 900 and 1300 cm^{-1} are characterized by a very similar shape, typical of thermally grown SiO_2 amorphous thin films.[32] These results confirm that Si in the films was always oxygen-saturated and that no sub-oxide was grown under any of the studied conditions. AFM measurements (not shown) of the film surface topography revealed the existence of few nanometer tall grains and surface roughness of 2.2 nm

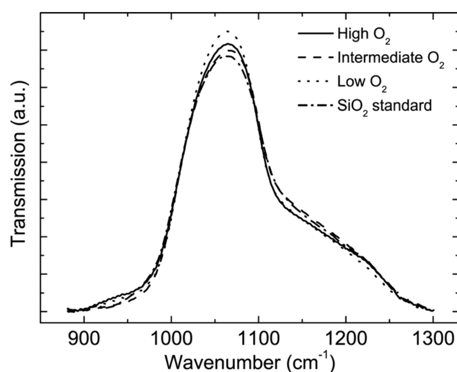

FIG. 4. Transmission infrared spectra of the three studied films, together with the spectrum of standard amorphous SiO_2 thin film.

in the case of the high O_2 pressure, 1.9 nm in the case of intermediate O_2 pressure, and 1.8 nm in the low O_2 pressure cases. Spectroscopic ellipsometry was used to determine the refractive indexes and, indirectly, the density of the films. Figure 5 shows that the refractive indexes of the different films as a function of the wavelength were in the order of that of a SiO_2 quartz crystal (with a refractive index of 1.53 for a wavelength of 500 nm), which indicates that, despite their amorphous structure, the films are quite dense. From their actual values of the refractive indexes, and using the Bruggeman model,[31] we obtained that void percentage for each film amounted to ∼0.7% in the case of high O_2 pressure, ∼5.8% for intermediate O_2 pressures and ∼6% for low O_2 pressures. This tendency indicates that films with vertical column-like coalescent structure (low and intermediate O_2 pressure cases) possess higher porosity than that of the film with the homogeneous microstructure (high O_2 pressure case). This also contrasts with the value 1.3 (for a wavelength of 500 nm) obtained for the refractive index of the film deposited at the backside of the substrate holder, and whose void percentage is 10.9%. Thus, despite the fact that Fig. 3(d) looks similar to those in Figs. 3(b) and 3(c), the lower value of the refractive index points toward a different concentration of pores and defects in this film, in agreement with the very different deposition conditions of growth.

The microstructural changes observed depicted in Figs. 3(a)–3(c) must be caused by a variation in the balance between the mechanisms governing the film growth. Regarding the SZM and the presence of the plasma, possible processes influencing the growth are[29] (i) the surface shadowing, (ii) the impingement of low energy positive ions, and (iii) the impingement of low and high energy negative ions. In this scheme, we do not consider thermally activated surface and bulk adatom diffusion since the value of T_s/T_m in all the studied conditions is below 0.2, i.e., the studied films grow in the Zone I of the SZM. In the following, we discuss the influence of the aforementioned processes trying to account for their relative importance in determining the different obtained microstructures.

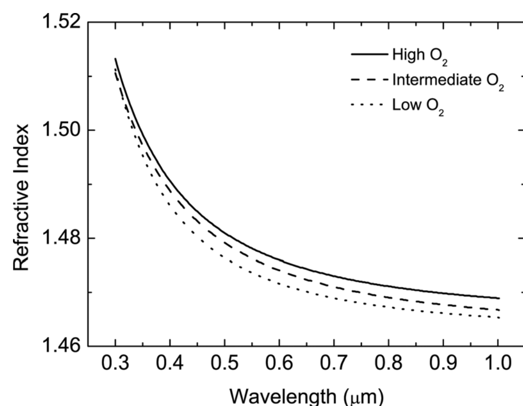

FIG. 5. Refractive indexes of the films deposited under the conditions appearing in Table I, as a function of the wavelength obtained by spectroscopic ellipsometry.

A. Surface shadowing

Sputtered Si atoms leave the cathode with a preferential direction and a high kinetic energy, typically of about 10 eV, and move through the plasma experiencing elastic and, in a lesser extent, inelastic collisions that make them lose kinetic energy and directionality. In general, an increase of the total pressure of the gases in the reactor implies a decrease of the mean free path of the Si atoms and, thus, more collisions, which ultimately lead toward the full thermalization of the sputtered particles with the heavy particles of the plasma. In previous publications we proved that, in absence of ion impingement and at low deposition temperatures (i.e., when surface shadowing governs the film growth), the higher the isotropy of the momentum distribution function of the sputtered particles in the plasma (or equivalently, the higher their thermalization degree), the more the growing film microstructure resembles that in Fig. 3(d).[16,22] Indeed, the growth of the film at the backside of the substrate holder takes place by the incorporation of Si sputtered atoms that have been (nearly) thermalized due to scattering processes in the plasma. This assumption is reasonable since, in average, only two collisions between sputtered Si and Ar atoms are required in order to lose the initial preferential directionality of the former.[15] Consequently, if surface shadowing governs the observed microstructural changes in Figs. 3(a)–3(c), higher total deposition pressures in the reactor would lead to the loss of the preferential directionality of the sputtered particles and, ultimately, to the appearance of vertical column-like structures (we disregard possible gas heating, since for magnetron sputtering of elements lighter than heavy particles in the plasma, in the working pressure range, it is a very weak effect[13,33]). This is, however, the opposite trend to that reported in Figs. 3(a)–3(c), where vertical structures disappear at the highest total pressure. Consequently, changes in the surface shadowing mechanism, associated to different total pressures in the deposition reactor, can be discarded as the main mechanism determining the microstructural changes reported in Figs. 3(a)–3(c).

B. Positive ion impingement

By using the mass-spectrometer, we have determined the characteristics of the positive ions moving toward the film. In agreement with the literature (see, for instance, Refs. 19 and 29) we have found that the positive argon ion flux, F_{Ar^+}, is several orders of magnitude above the flux of

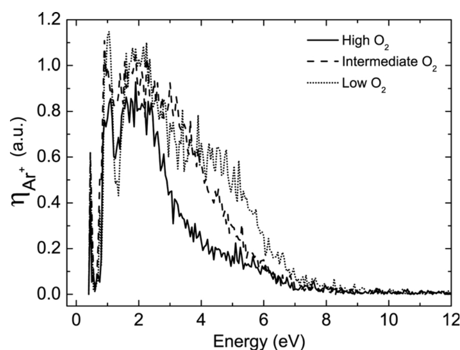

FIG. 6. η_{Ar^+} as a function of the energy in the conditions in Table I.

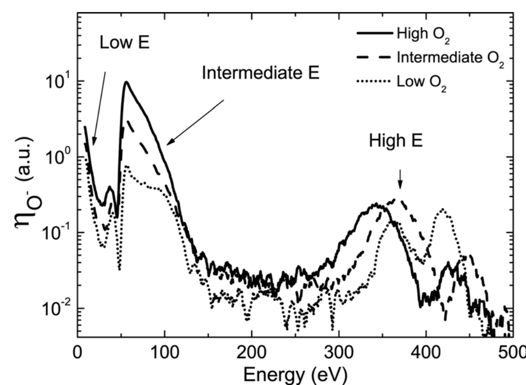

FIG. 7. η_{O^-} as a function of the energy in the conditions in Table I.

any other positive ion (not shown). The key quantity to account for the role of these ions is given by the non-dimensional quantity $\eta_{Ar^+} = F_{Ar^+}/r_d$, where r_d is the deposition rate.[23] In Fig. 6 we present the value of η_{Ar^+} for the three studied depositions conditions as a function of the ion energy: in all the cases, their kinetic energy was below 10 eV, corresponding to the energy gained by the ions when accelerated in the mass spectrometer detector's sheath. For the ions reaching the film surface we expect same spectra with a shift of few electronvolts as substrates are at floating potential, i.e., not grounded. This distribution of impinging ions results in the following energy-integrated values of η_{Ar^+} (in arbitrary units), $\eta_{Ar^+}(\text{high}O_2) = 0.64$, η_{Ar^+}(intermediate O_2) $= 0.92$ and $\eta_{Ar^+}(\text{low}O_2) = 1$, which means that the influence of the Ar^+ impingement on the film decreases with the O_2 pressure. As mentioned in the Introduction, ion bombardment causes the removal of geometrical patterns and the densification of the thin films thanks to the enhancement surface adatom mobility (see, for instance, Refs. 19, 23 and 27). Regarding the obtained values of η_{Ar^+}, if positive ion impingement was responsible for the microstructural changes observed in Figs. 3(a)–3(c), we would find that for the lower O_2 pressure (higher values of η_{Ar^+}), the film would depict less geometrical vertical structures and be more dense than in the high O_2 case, which is indeed the opposite behavior to that actually found. Consequently, Ar^+ impingement on the film cannot either be the main factor accounting for the observed microstructural changes.

C. Negative ion impingement

For the negative ions, in agreement with data in the literature,[21,25,26] we have found that the most important negative ion flux is that of O^- ions which, throughout the whole energy range analyzed, is several orders of magnitude higher than that of O_2^-, SiO_2^-, SiO_3^-, etc. ions (not shown). The measured energy spectra of the O^- ions, reported in Fig. 7, are characterized by several peaks appearing at different energies. In the low energy range we found a small peak at a similar kinetic energy as the positive ions (i.e., below 20 eV). Next, we obtained several peaks at energies ranging from about 20 eV to 200 eV: they are explained in the literature by considering oxygen-containing negative molecular ions that, being produced at the cathode, are subsequently dissociated in the plasma, splitting the kinetic energy according to the relative masses of the fragments.[29] In our case, the peak starting at about 50 eV indicates that either the production of heavy negative ions could be relevant or that lighter negative ions might be produced in the neighborhood of the cathode via electron attachment, thus possessing less energy than those generated on the cathode surface. The discussion on which of the two abovementioned mechanisms is responsible for the generation of these intermediate energy oxygen ions is far from the scope of this paper, although the existence of these ions is clearly demonstrated in Fig. 7, a fact that was already reported in Ref. 30. Finally, at high energies (above 200 eV) we find two main peaks just below and above the cathode potential in each case: they correspond to O^- ions produced on the cathode that passed through the orifice of the mass spectrometer. The two peak structure is generated because the plasma is maintained by a pulsed dc generator, well known for possessing two different regimes during the "on" period of the electromagnetic signal.[24] Again, the magnitude that can be used to account for the relative importance of these ions on the formation of the film microstructure is given by the non-dimensional quantity $\eta_{O^-} = F_{O^-}/r_d$, where F_{O^-} is the flux of O^- ions.[23] The energy-integrated values in the cases of low, intermediate, and high O_2 pressures are reported in Fig. 8, showing that this parameter attains higher values for increasing O_2 pressures. In Fig. 8 we have also reported the trend found for the low energy (between 0 and 20 eV), intermediate energy (between 20 and 200 eV), and high energy (above 200 eV) O^- ions. It appears that the most important contribution corresponds to O^- ions in the intermediate energy range, whereas the high and low energy range contributions are much lower. In agreement with Ref. 23, a higher value of η_{O^-} would involve a higher adatom surface mobility, the densification of the material as well as the removal of bulk patterns. Hence, the trend reported in Fig. 8 agrees with that found in Figs. 3(a)–3(c), and, consequently, among the processes involved in the formation of the microstructure of the films, only the trend followed by the O^- impingement on the film surface, and particularly of O^- ions with energies between 20 and 200 eV, agrees with the reported changes. Interestingly, regarding Fig. 7, the observed changes in the SiO_2 microstructure are not related to an increase of the ion kinetic energy, but rather to an increase of the O^- impingement rate.

The results presented in this paper agree with Ref. 34 where it is found that, for a very wide range of ion fluxes,

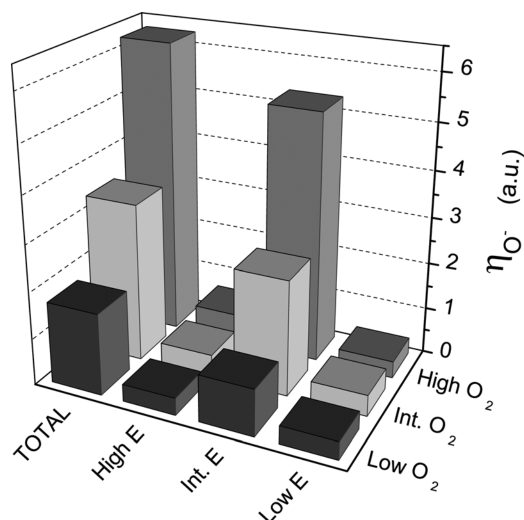

FIG. 8. Energy integrated value of η_{O^-}: Total value, low energy contribution (below 20 eV), intermediate energy contribution (between 20 and 200 eV), and high energy contribution (above 200 eV).

ion impingement during growth with kinetic energies around 10 eV affected very little the orientation development of crystalline planes of NaCl-structure $\delta-$TaN layers, whereas ion energies above 20 eV strongly modified the structure of the films. This energy is related to typical adatom surface transport threshold energies, and agrees with our conclusions that ion impingement, with energy below 10 eV (see Fig. 6), is not responsible for the microstructural changes reported in Figs. 3(a)–3(c). Overall, by considering the discussion above, we have demonstrated that, despite cathode poisoning, O_2 content in the plasma influences the deposited SiO_2 film microstructure and revealed the existence of two growth regimes controlled by the amount of O_2 in the deposition reactor, linked to the competition between ion-induced adatom surface mobility and the surface shadowing mechanism.

IV. CONCLUSIONS

Microstructural changes of amorphous SiO_2 thin films deposited by reactive magnetron sputtering at low temperatures have been studied. Three deposition conditions have been analyzed that involved different ion fluxes and film microstructures. Coalescent vertical column-like structures were found in the film for low and intermediate O_2 pressures in the deposition reactor. These structures vanished for the highest O_2 pressure case, resulting in a homogeneous film. The main processes governing the growth and responsible for the microstructural changes in the material in our conditions are discussed: surface shadowing, dependent on the deposition particle directionality when arriving at the film surface, positive ion impingement, and negative ion impingement. Among these processes, only the trend followed by the negative ion impingement, and, in particular, the impingement of O^- ions with kinetic energies between 20 and 200 eV agrees with the transition from a vertical coalescent column-like microstructure to a more dense homogeneous film.

Overall, we have shown the existence of two growth regimes at low temperatures, controlled by the amount of O_2 in the deposition reactor, and caused by the competition between surface shadowing and ion-induced adatom surface mobility processes.

ACKNOWLEDGMENTS

J.C.G. thanks CSIC for his JAE-Doc contract (2009-2012) at the ICMS-CSIC-US (Spain). Financial support from the Spanish Ministry of Innovation (Projects No. MAT 2007-65764 and CONSOLIDER INGENIO 2010-CSD2008-00023) and the Junta de Andalucía (Project Nos. TEP2275, TEP5283, P07-FQM-03298, and P10-FQM-6900) is acknowledged. We would like to thank Dr. F. Yubero for his help.

[1]K. M. Pollock, T. Kaufman-Osborn, J. Hiltrop, and J. R. Doyle, J. Vac. Sci. Technol. A **29**, 051301 (2011).
[2]K. Ellmer, J. Phys. D: Appl. Phys. **33**, 17, (2000).
[3]Y. Matsuda, Y. Yamori, S. Ohgushi, M. Muta, and H. Fujiyama, Surf. Coat. Technol. **98**, 1286 (1998).
[4]P. J. Kelly and R. D. Arnell, Vacuum **56**, 159 (2000).
[5]A. Bogaerts, E. Bultinck, M. Eckert, V. Georgieva, M. Mao, E. Neyts, and L. Schwaederle, Plasma Process. Polym. **6**, 295 (2009).
[6]A. Palmero, N. Tomozeiu, A. M. Vredenberg, W. M. Arnoldbik, and F. H. P. M. Habraken, Surf. Coat. Technol. **177–178**, 215 (2004).
[7]S. Mráz and J. M. Schneider, J. Appl. Phys. **109**, 023512 (2011).
[8]J. Sun, Y. Huang, and H. Gong, J. Appl. Phys. **110**, 023709 (2011).
[9]S. Zhang, D. Sun, Y. Fu, and H. Du, Surf. Coat. Technol. **167**, 113 (2003).
[10]I. Safi, Surf. Coat. Technol. **127**, 204 (2000).
[11]R. Snyders, J.-P. Dauchot, and M. Hecq, Plas. Proc. Poly. **4**, 113 (2007).
[12]C. Vitelaru, L. de Poucques, T. Hytkova, T. M. Minea, C. Boise-Laporte, J. Bretagne, and G. Popa, Plas. Proc. Poly. **6**, 326 (2009).
[13]A. Palmero, H. Rudolph, and F. H. P. M. Habraken, Appl. Phys. Lett. **87**, 071501 (2005).
[14]A. Palmero, H. Rudolph, and F. H. P. M. Habraken, Appl. Phys. Lett. **89**, 211501 (2006).
[15]A. Palmero, H. Rudolph, and F. H. P. M. Habraken, J. Appl. Phys. **101**, 083307 (2007).
[16]R. Alvarez, P. Romero-Gomez, J. Gil-Rostra, J. Cotrino, F. Yubero, A. Palmero, and A. R. Gonzalez-Elipe, J. Appl. Phys. **108**, 064316 (2010).
[17]E. D. van Hattum, A. Palmero, W. M. Arnoldbik, H. Rudolph, and F. H. P. M. Habraken, Appl. Phys. Lett. **91**, 171501 (2007).
[18]A. C. Sun, F. T. Yuan, J.-H. Hsu, W. M. Liao, and H. Y. Lee, J. Appl. Phys. **105**, 07B719 (2009).
[19]P. Kudlácek, J. Vlcek, J. Houska, J. G. Han, M. J. Jung, and Y. M. Kim, Vacuum **81**, 1109 (2007).
[20]L. P. Wang, K. Y. Fu, X. B. Tian, B. Y. Tang, and P. K. Chu, Mater. Sci. Eng. A **336**, 75 (2002).
[21]T. Welzel, S. Naumov, and K. Ellmer, J. Appl. Phys. **109**, 073302 (2011).
[22]J. M. García-Martín, R. Alvarez, P. Romero-Gómez, A. Cebollada, and A. Palmero, Appl. Phys. Lett. **97**, 173103 (2010).
[23]I. Petrov, P. B. Barna, L. Hultman, and J. G. Greene, J. Vac. Sci. Technol. A **21**, 117, (2003).
[24]M. Misina, J. W. Bradley, H. Backer, Y. Aranda-Gonzalvo, S. K. Karkari, and D. Forder, Vacuum **68**, 171 (2003).
[25]P. Pokorny, M. Misina, J. Bulir, J. Lancok, P. Fitl, J. Musil, and M. Novotny, Plas. Proc. Pol. **8**, 459 (2011).
[26]N. Tsukamoto, D. Watanabe, M. Saito, Y. Sato, N. Oka, and Y. Shigesato, J. Vac. Sci. Technol. **28**, 846 (2010).
[27]R. Messier, A. P. Giri, and R. A. Roy, J. Vac. Sci. Technol. A **2**, 500 (1984).
[28]A. Anders, Thin Solid Films **518**, 4087 (2010).
[29]M. Zeuner, H. Neumann, J. Zalman, and H. Biederman, J. Appl. Phys. **83**, 5083 (1998).
[30]S. Mráz and J. M. Schneider, J. Appl. Phys. **100**, 023503 (2006).
[31]D. A. G. Bruggeman, Ann. Phys., **24**, 636 (1935).
[32]A. Barranco, F. Yubero, J. Cotrino, J. P. Espinos, J. Benitez, T. C. Rojas, J. Allain, T. Girardeau, J. P. Riviere, and A. R. Gonzalez-Elipe, Thin Solid Films **396**, 9 (2001).
[33]A. Palmero, H. Rudolph, and F. H. P. M. Habraken, Thin Solid Films **515**, 631 (2006).
[34]C.-S Shin, D. Gall, T.-W. Kim, N. Hellgren, I. Petrov, and J. E. Greene, J. Appl. Phys. **92**, 5084 (2002).